Title
SNX27 mediates PDZ-directed sorting from endosomes to the plasma membrane.

Journal
The Journal of cell biology, 190(4)

ISSN
0021-9525

Authors
Lauffer, Benjamin EL
Melero, Cristina
Temkin, Paul
et al.

Publication Date
2010-08-01

DOI
10.1083/jcb.201004060

Peer reviewed

SNX27 mediates PDZ-directed sorting from endosomes to the plasma membrane

Benjamin E.L. Lauffer,[1] Cristina Melero,[2] Paul Temkin,[3,4] Cai Lei,[7] Wanjin Hong,[7] Tanja Kortemme,[2] and Mark von Zastrow[3,5,6]

[1]Program in Pharmaceutical Sciences and Pharmacogenomics, [2]Department of Bioengineering and Therapeutic Sciences, [3]Program in Cell Biology, [4]Department of Biochemistry and Biophysics, [5]Department of Psychiatry, and [6]Department of Cellular and Molecular Pharmacology, University of California, San Francisco, San Francisco, CA 94158
[7]Membrane and Biology Laboratory, Institute of Molecular and Cell Biology, Singapore 138673

Postsynaptic density 95/discs large/zonus occludens-1 (PDZ) domain–interacting motifs, in addition to their well-established roles in protein scaffolding at the cell surface, are proposed to act as cis-acting determinants directing the molecular sorting of transmembrane cargo from endosomes to the plasma membrane. This hypothesis requires the existence of a specific trans-acting PDZ protein that mediates the proposed sorting operation in the endosome membrane. Here, we show that sorting nexin 27 (SNX27) is required for efficient PDZ-directed recycling of the β_2-adrenoreceptor (β_2AR) from early endosomes. SNX27 mediates this sorting function when expressed at endogenous levels, and its recycling activity requires both PDZ domain–dependent recognition of the β_2AR cytoplasmic tail and Phox homology (PX) domain–dependent association with the endosome membrane. These results identify a discrete role of SNX27 in PDZ-directed recycling of a physiologically important signaling receptor, and extend the concept of cargo-specific molecular sorting in the recycling pathway.

Introduction

The β_2-adrenoreceptor (β_2AR) is a member of the large family of G protein–coupled signaling receptors (GPCRs), and is fundamentally regulated by ligand-induced endocytosis via clathrin-coated pits (Moore et al., 2007). The functional consequences of regulated endocytosis, specifically whether catecholamines produce sustained or transient effects, are determined by molecular sorting of internalized β_2ARs between recycling and lysosomal pathways (Hanyaloglu and von Zastrow, 2008; Marchese et al., 2008). β_2ARs recycle efficiently to the plasma membrane after endocytosis, but, in contrast to the ability of some endocytic cargo to recycle essentially by bulk membrane flux, efficient recycling of the β_2AR requires a postsynaptic density 95/discs large/zonus occludens-1 (PDZ) domain–interacting motif present in its distal cytoplasmic tail (Maxfield and McGraw, 2004; Hanyaloglu et al., 2005). If this motif is disrupted by phosphorylation or mutation, internalized β_2ARs traffic preferentially to lysosomes and are degraded (Cao et al., 1999; Gage et al., 2001). The β_2AR-derived recycling motif can bind to a family of PDZ proteins related to Ezrin-binding phosphoprotein of 50 kD (EBP50) or Na^+/H^+ exchange regulatory factor (NHERF; Hall et al., 1998; Cao et al., 1999; He et al., 2006). These observations, and results from the study of other PDZ motif–bearing GPCRs (Wente et al., 2005; Delhaye et al., 2007; Hanyaloglu and von Zastrow, 2008), have motivated the hypothesis that PDZ motifs mediate a discrete endosome-to-plasma membrane sorting operation (Gage et al., 2005; Wang et al., 2007).

A problem with the PDZ-directed recycling hypothesis is that NHERF family PDZ proteins, although often concentrated in the cortical cytoplasm near endosomes, are not known to localize directly to the endosome membrane when expressed at endogenous levels (Bretscher et al., 2000; Donowitz et al., 2005), and can mediate additional effects on receptors (Hall et al., 1998). It is also known that PDZ domain–mediated interactions

Correspondence to Mark von Zastrow: mark.vonzastrow@ucsf.edu

Abbreviations used in this paper: β_2AR, β_2-adrenoreceptor; EBP50, Ezrin-binding phosphoprotein of 50 kD; GPCR, G protein–coupled receptor; mrs, μ receptor–derived recycling sequence; NHERF, Na^+/H^+ exchange regulatory factor; PDZ, postsynaptic density 95/discs large/zonus occludens-1; SNX27, sorting nexin 27.

The Rockefeller University Press $30.00
J. Cell Biol. Vol. 190 No. 4 565–574
www.jcb.org/cgi/doi/10.1083/jcb.201004060

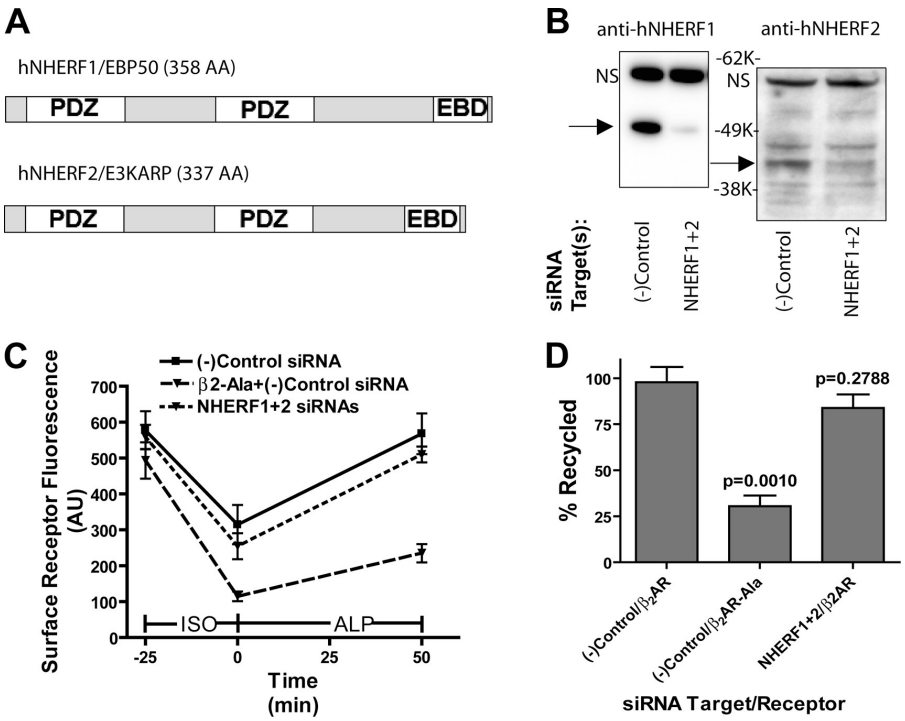

Figure 1. **Efficient internalization and recycling of the β_2AR in HEK293 cells simultaneously depleted of NHERFs 1 and 2.** (A) Schematic of NHERF1 (also called EBP50) and NHERF2 (also called E3KARP) domain organization, showing PDZ domains and ERM protein-binding domain (EBD). (B) Verification of dual NHERF1 + 2 knockdown by immunoblotting. Arrows indicate specific bands; nonspecific bands (NS) verify equal loading between the indicated samples. Molecular mass markers (in kilodaltons) are indicated. Images shown are representative of three experiments. (C) Flow cytometric assessment of receptor internalization and recycling. HEK293 cells stably expressing either FLAG-tagged, wild-type β_2AR, or the FLAG-β_2AR-Ala PDZ mutant were transfected with the indicated siRNAs and assayed for surface receptor immunoreactivity before and after an agonist pretreatment and washout using fluorescence flow cytometry. (D) Recycling efficiency calculated from data shown in C, as described in Materials and methods. All error bars indicate SEM. P-values: Student's *t* test with the negative control condition; $n = 3$ or 4.

with various membrane proteins can enhance net surface accumulation indirectly, such as by scaffold-promoted posttranslational modification (Gardner et al., 2007) or physical stabilization of proteins in particular plasma membrane domains (Perego et al., 1999). A critical unresolved question, therefore, is whether there exists any trans-acting PDZ protein that sorts relevant motif-bearing cargo into the recycling pathway directly from the endosome membrane.

Such a bona fide sorting protein for the PDZ-directed recycling pathway, if it exists, would be expected to possess several key properties. First, of course, the putative sorting protein should be capable of binding the relevant cis-acting PDZ motif. Second, the putative sorting protein should localize to, or physically interact with, endosomes traversed by the internalized cargo. Third, the putative sorting protein should be essential for PDZ-directed recycling when expressed at endogenous levels. Fourth, and most important for establishing a direct endosome-based sorting function, the recycling activity of the putative sorting protein should require both binding to the cis-acting PDZ motif and localization to the relevant endosomes from which recycling occurs. Here, we show that sorting nexin 27 (SNX27) meets all of these criteria, and that this PDZ protein plays an essential role regulating the β_2AR.

Results and discussion

Two NHERF family PDZ proteins that bind the β_2AR tail, NHERF1 and NHERF2, are not known to localize to endosomes at steady state, but possess a C-terminal Ezrin/Radixin/Moesin (ERM) protein-binding domain (Fig. 1 A) that can mediate a network of protein connectivity linking integral membrane proteins to actin (Bretscher et al., 2000). We initially proposed such indirect actin connectivity as the basis for β_2AR recycling (Cao et al., 1999). Subsequent analysis established that, although actin connectivity is sufficient to promote recycling of engineered receptors in the absence of a natural PDZ motif, this connectivity does not fully recapitulate the natural characteristics of β_2AR recycling (Lauffer et al., 2009). As such, we sought to test whether or not NHERFs 1 and/or 2 are actually the limiting factors for β_2AR recycling. To do so, we used an established HEK293 cell clone expressing a FLAG-tagged β_2AR construct and depleted both NHERF family proteins simultaneously using a mixture of RNA duplexes (Fig. 1 B). We then applied a fluorescence flow cytometric assay to measure receptor internalization occurring in response to application of the adrenergic agonist isoproterenol (10 µM), and recycling of receptors after subsequent washout of this agonist (Fig. 1 C). As shown previously, surface β_2AR immunoreactivity recovered nearly to control levels within 50 min after agonist removal (Fig. 1 C, solid line; Cao et al., 1999), whereas surface recovery of an alanine-extended (PDZ binding defective) mutant receptor construct (β_2AR-Ala) was greatly reduced (Fig. 1 C, broken line). Calculation of fractional recycling (Hanyaloglu et al., 2005) confirmed this effect across multiple experiments (Fig. 1 D, left and middle bars). Strikingly, simultaneous knockdown of NHERFs 1 and 2 did not have a major effect on β_2AR recycling when compared with control levels (Fig. 1 D, first and third bars). Consistent with this, we also observed PDZ motif–dependent recycling of the β_2AR in a cell line (PS120) that expresses NHERF proteins at low levels (Donowitz et al., 2005) relative to HEK293 cells (unpublished data).

Thus, we considered whether another PDZ protein might function alternately, or additionally, in endosome-to-plasma membrane trafficking of β_2ARs. An intriguing candidate was SNX27 (also called Mrt1), which is widely expressed and unique among PDZ proteins because it contains a PX domain

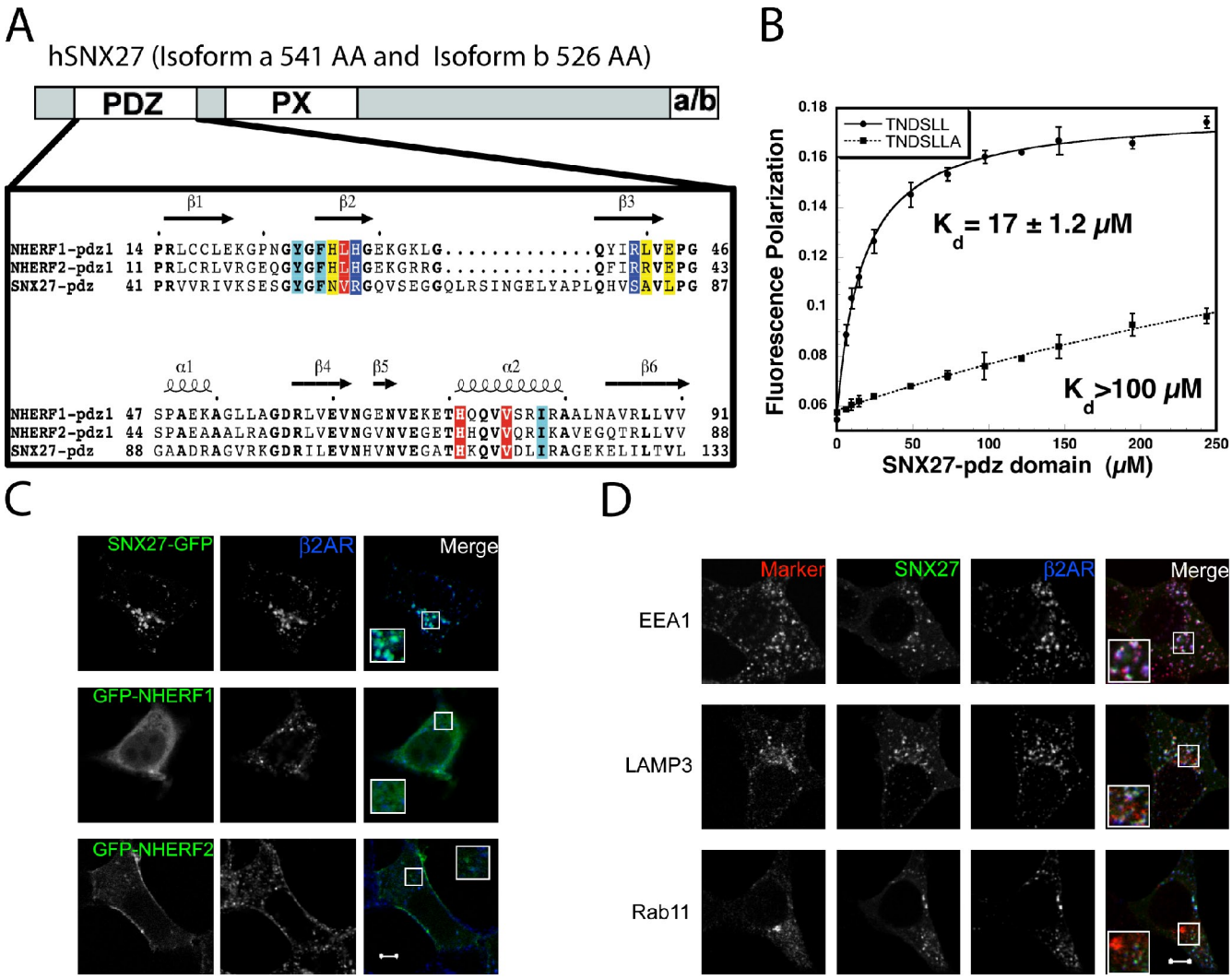

Figure 2. **SNX27 is a distinct NHERF-related PDZ protein that interacts with the β_2AR in early endosomes.** (A) Schematic of SNX27 domain organization showing the PDZ domain, the PX domain, and the alternatively spliced C-terminal region that distinguishes a and b isoforms of SNX27 (a/b). Expanded box shows sequence comparison of the SNX27 PDZ domain (residues 43–133) with the first PDZ domain of NHERF1 (residues 14–91) and NHERF2 (residues 11–88). Sequences obtained from the Swiss/UniProt database were aligned with ClustalW (Thompson et al., 1994) and displayed with ESPript (Gouet et al., 1999). Secondary structure elements of the first PDZ domain of NHERF1 (Protein Data Bank accession No. 1g9o) are indicated above the alignment. Conserved residues in the three PDZ domains are shown in bold. Residues critical for recognition of peptide side chains at positions P_0, P_{-1}, P_{-2}, and P_{-3} are shown in cyan, yellow, red, and blue, respectively (Appleton et al., 2006). (B) Interaction of the β_2AR-derived tail sequence with the SNX27-derived PDZ domain. Purified, recombinant PDZ domain was mixed in increasing concentration with FITC-labeled peptides corresponding to the six C-terminal residues of the wild-type β_2AR (a transplantable recycling sequence, solid line), or an alanine-extended version that lacks detectable recycling activity (broken line). K_d was estimated by single site fit. The plots shown are representative of three independent experiments; error bars reflect a representative SD of triplicate samples. (C) FLAG-β_2AR–expressing HEK293 cells were transfected with the indicated GFP-tagged PDZ protein. After internalization of antibody-labeled receptors stimulated by 10 μM isoproterenol for 25 min, cells were fixed and imaged using dual-channel, laser-scanning confocal microscopy to reveal subcellular localization of the indicated protein. (D) FLAG-β_2AR– and SNX27-GFP–transfected cells were further stained for endocytic markers that were imaged in a third fluorescent channel. All images show a middle z section and are representative of at least three independent experiments. Merged images contain boxed insets enlarged 2× from the indicated regions. Bars, 5 μm.

that binds specifically to phosphatidylinositol 3-phosphate enriched on the cytoplasmic surface of early/sorting endosomes (Lunn et al., 2007; Rincón et al., 2007). SNX27 has not been shown previously to interact with the β_2AR's PDZ motif, but sequence analysis suggests a close relationship between SNX27's PDZ domain and those present in NHERF family proteins (Fig. 2 A, bold residues; Donowitz et al., 2005). In particular, we noted similarity or identity at several residues thought to directly contact the PDZ motif (colored residues; Appleton et al., 2006). Consistent with this, equilibrium binding analysis using fluorescence polarization demonstrated direct and saturable binding of this motif (a peptide corresponding to the C-terminal six residues of the β_2AR) to the purified SNX27 PDZ domain (Fig. 2 B, solid line; equilibrium dissociation constant K_d = 17 ± 1.2 μM). Further, binding to the SNX27 PDZ domain in vitro was destabilized by the alanine extension that blocks the recycling activity of this sequence in intact cells (Fig. 2 B, dotted line; K_d > 100 μM).

We next asked if full-length SNX27 associates with endosomes traversed by internalized β_2ARs. To do so, we expressed a

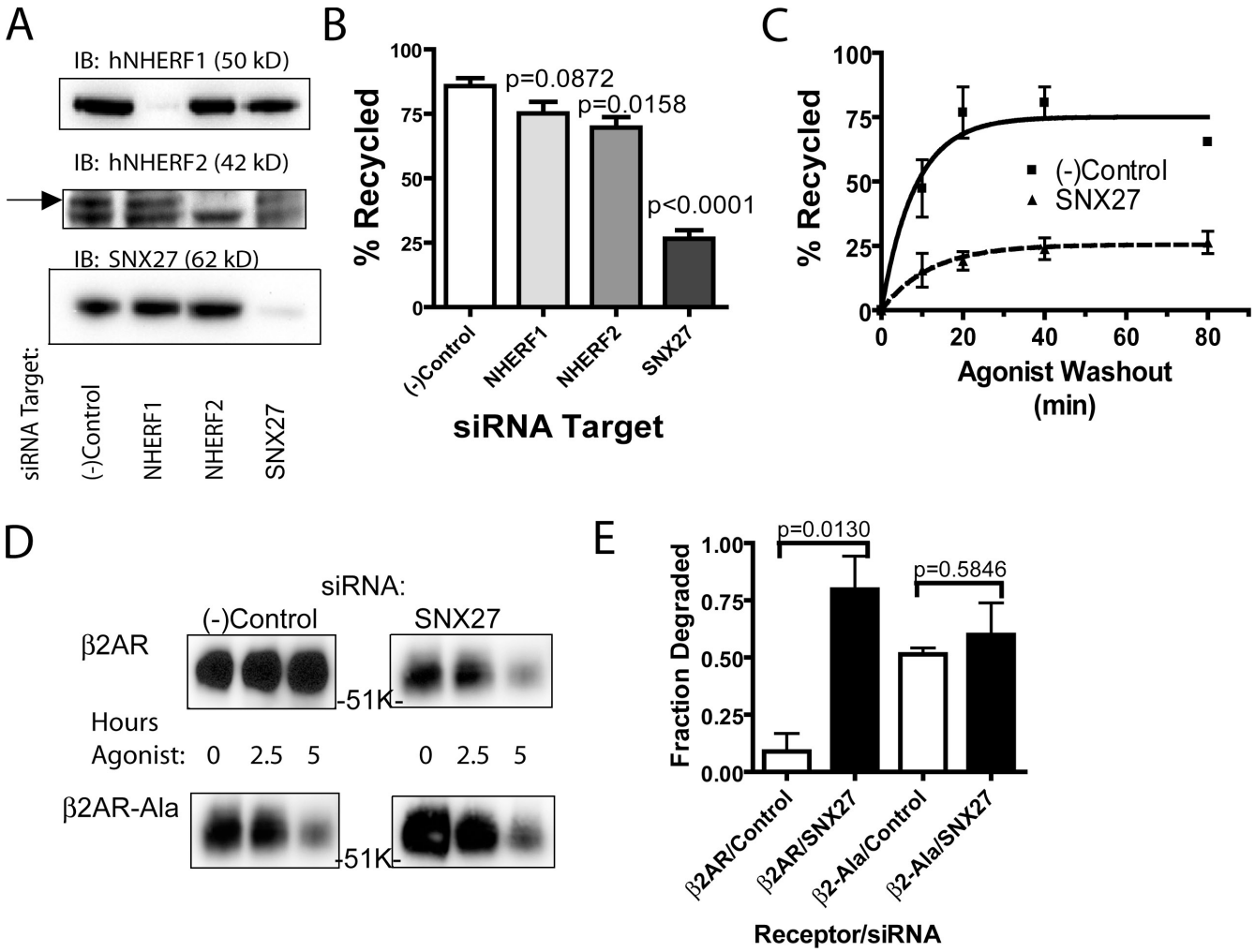

Figure 3. **Depletion of endogenous SNX27 prevents PDZ-directed recycling of β_2ARs and accelerates down-regulation.** (A) Representative immunoblot analysis (n = 4) of siRNA-mediated knockdown of the indicated PDZ protein in β_2AR-expressing HEK293 cells. NHERF2 (arrow) resolves above a nonspecific band that verifies equal loading. Apparent molecular masses are indicated in parentheses. (B) Effect of knockdowns on FLAG-β_2AR recycling assessed by fluorescence flow cytometry 50 min after agonist removal from the culture medium. Error bars indicate SEM. P-values: Student's t test with negative control results; n = 4–6. (C) Time course of FLAG-β_2AR recycling in cells transfected with control (solid line) compared with SNX27 siRNA (broken line). Error bars indicate SEM; n = 4. (D) Effect of SNX27 depletion on turnover of surface-biotinylated FLAG-β_2AR (top) and FLAG-β_2AR-Ala (bottom) after incubation of cells for the indicated time period with 10 µM isoproterenol. K, kilodaltons. (E) Quantification of the loss of biotinylated, FLAG-tagged receptors after the 5-h exposure to 10 µM isoproterenol. Error bars indicate SEM. P-values: Student's t test for the SNX27 effect on degradation for each receptor; n = 3.

GFP-tagged version of SNX27a in the FLAG-β_2AR–expressing HEK293 cell clone used for trafficking studies. We then exposed these cells to 10 µM isoproterenol for 25 min in the presence of Alexa Flour–conjugated M1 anti-FLAG monoclonal antibody to drive fluorescently tagged β_2ARs to steady state throughout the recycling pathway (Gage et al., 2001). SNX27-GFP localized prominently to endosomal membranes, as shown previously (Joubert et al., 2004; Lunn et al., 2007; Rincón et al., 2007), and a large fraction of these endosomes contained internalized β_2ARs (Fig. 2 C, top). We quantified this observation by counting the number of β_2AR-containing endosomes colocalized with SNX27 in coded specimens (90% overlap, 8,586 endosomes, 124 cells, three experiments). We additionally verified extensive overlap by determining Pearson's correlation coefficient between the respective image channels (0.62 ± 0.09, n = 12 images). In contrast, GFP-tagged NHERF1 was distributed throughout the cytoplasm with visible enrichment near the plasma membrane, but we did not observe or measure significant endosome localization (Fig. 2 C, second row of images; a different focal plane showing enrichment near the plasma membrane is shown in Fig. S1 A; Pearson's coefficient = 0.33 ± 0.15; n = 12). GFP-NHERF2 was enriched near the plasma membrane but also localized to a fraction of β_2AR-containing endosomes (Fig. 2 C, bottom). The fluorescence intensity of GFP-NHERF2 on endosomes was not high, however (Pearson's coefficient = 0.29 ± 0.15; n = 12), and GFP-NHERF2 colocalization was visible only when β_2ARs were also present (Fig. S1 B, second row from the top, compare left and right image pairs). SNX27-GFP was unique in localizing prominently to endosomes either in the absence or presence of β_2ARs (Fig. S1 B, bottom two rows). The SNX27-associated endosomes colocalized extensively with EEA1 (Fig. 2 D, top; 92% overlap, 4,119 endosomes, 54 cells, three experiments; Pearson's coefficient = 0.60 ± 0.14; n = 28 images). In contrast, we observed little

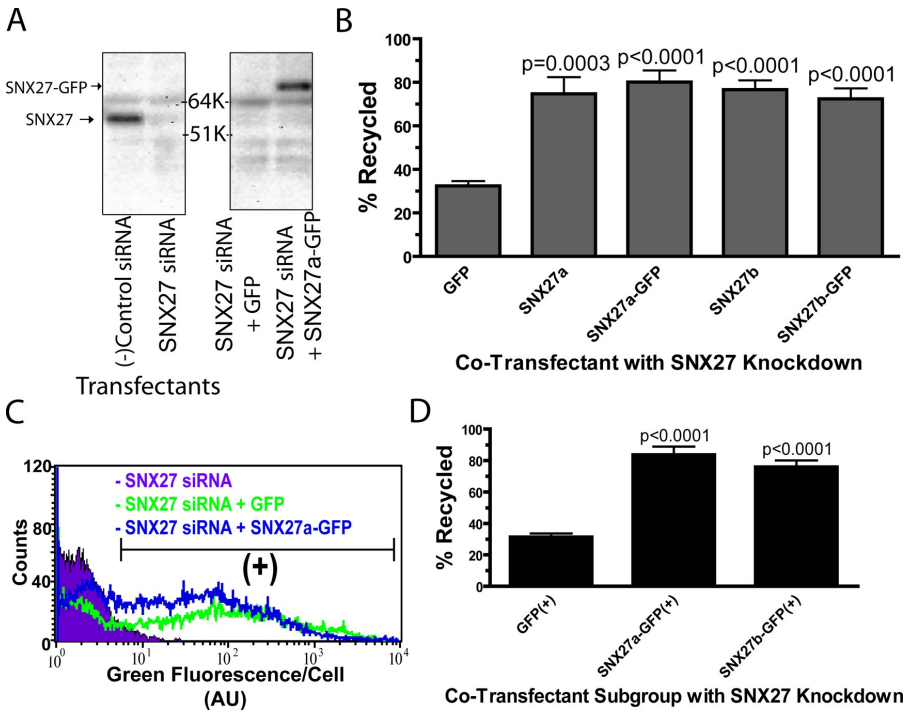

Figure 4. **Transgenic rescue of β_2AR recycling by recombinant SNX27.** (A) Immunoblot showing depletion of endogenous SNX27 by silencing relative to negative control siRNA (lanes 1 and 2), and replacement by cotransfection of SNX27-GFP but not GFP control plasmid (lanes 3 and 4). Electrophoretic mobilities of endogenous and SNX27 and recombinant SNX27-GFP are indicated by arrows. K, kilodaltons. (B) Flow cytometric analysis showing rescue of FLAG-β_2AR recycling in SNX27 knockdown cells by cotransfection of either isoform of recombinant rat SNX27, or their GFP-tagged counterparts. (C and D) Verification of transgenic rescue using dual-channel fluorescence flow cytometry and gating of recycling data based on recombinant SNX27 expression. (C) A representative fluorescence intensity histogram of the GFP channel. The region indicated by (+) represents the populations used to verify transgenic rescue of recycling. (D) FLAG-β2AR recycling measured specifically in the SNX27/GFP (+) population. Error bars indicate SEM. P-values: Student's *t* test with GFP control; n = 4–6 experiments.

overlap with LAMP3 or with Rab11 (Fig. 2 D, middle and bottom; Pearson's coefficient = 0.38 ± 0.16 [n = 28] and 0.25 ± 0.10 [n = 27]). These observations define the SNX27-associated membrane compartments primarily as early endosomes.

We next applied RNA interference to test the functional significance of candidate PDZ proteins when knocked down individually (Fig. 3 A). Consistent with the dual-knockdown results, depletion of NHERF1 did not significantly affect β_2AR recycling (Fig. 3 B, compare first and second bars from the left). Depletion of NHERF2 produced a significant inhibition of β_2AR recycling, but the magnitude of this effect was small (Fig. 3 B, third bar from the left). Depletion of SNX27, in contrast, caused a pronounced inhibition of β_2AR recycling (Fig. 3 B, rightmost bar) that was similar in magnitude to the effect of disrupting the cis-acting PDZ motif itself (β_2AR-Ala mutant receptor; Fig. 1 D). Pronounced inhibition of β_2AR recycling in SNX27-depleted cells was further verified by visual inspection of epifluorescence micrographs (Fig. S1 C).

SNX27 knockdown increased net receptor internalization measured at a steady state, which is consistent with the ability of β_2ARs to repeatedly endocytose and recycle in the continuous presence of an agonist (von Zastrow and Kobilka, 1992). Kinetic analysis indicated that increased net receptor internalization was accounted for by the reduced fractional recycling of receptors (F_r) produced by SNX27 depletion (Figs. 3 C and S2 C). Also supporting this interpretation, surface biotinylation and immunoblot analysis established that SNX27 knockdown increased agonist-induced proteolysis of the β_2AR (Fig. 3, D and E). Further, SNX27 depletion produced a net downregulation of surface and total cellular receptor number measured by fluorescence flow cytometry and a radioligand binding assay, respectively, in cells maintained in the absence of agonist (Fig. S2, A and B). All of these observations are consistent with the hypothesis that SNX27, by mediating PDZ-directed sorting of internalized β_2ARs into the rapid recycling pathway, effectively prevents receptors from trafficking to lysosomes after both basal and agonist-stimulated endocytosis.

To further verify the specificity of the SNX27 knockdown effect, we investigated rescue using rat-derived SNX27 constructs not targeted by the human-specific siRNA duplexes. Selective knockdown and replacement were confirmed by anti-SNX27 immunoblotting (Fig. 4 A). Both a and b isoforms of SNX27, which differ by alternative splicing affecting the C-terminal 15 residues (Kajii et al., 2003), effectively rescued β_2AR recycling, whereas control expression of GFP did not (Fig. 4 B). We also verified rescue of net surface receptor immunoreactivity when measured at steady state in the absence of agonist (unpublished data). Gating the flow cytometric analysis according to GFP signal (Fig. 4 C) further verified transgenic rescue of β_2AR recycling by both SNX27 isoforms over a range of expression levels (Fig. 4 D).

We next asked if the recycling activity of SNX27 requires its ability to bind the PDZ motif present in the β_2AR tail. To do so, we mutated a single conserved histidine residue present in the second α helix of the SNX27 PDZ domain (position 112 in rat SNX27 corresponds to position 114 in human, highlighted in red in Fig. 2 A), which is predicted to form a critical hydrogen bond with the Ser/Thr residue located at the −2 position of the PDZ-interacting motif (corresponding to S411 of the human β_2AR; Doyle et al., 1996; Tonikian et al., 2008). This point mutation destabilized binding of SNX27 to the β_2AR-derived sorting motif (Fig. 5 A), and did so to a similarly large degree as mutating the PDZ motif itself (compare to Fig. 2 B). Using circular dichroism and gel filtration, we ruled out changes in PDZ fold stability or oligomerization state as an explanation for this result (unpublished data). Further, the H112A mutation did not

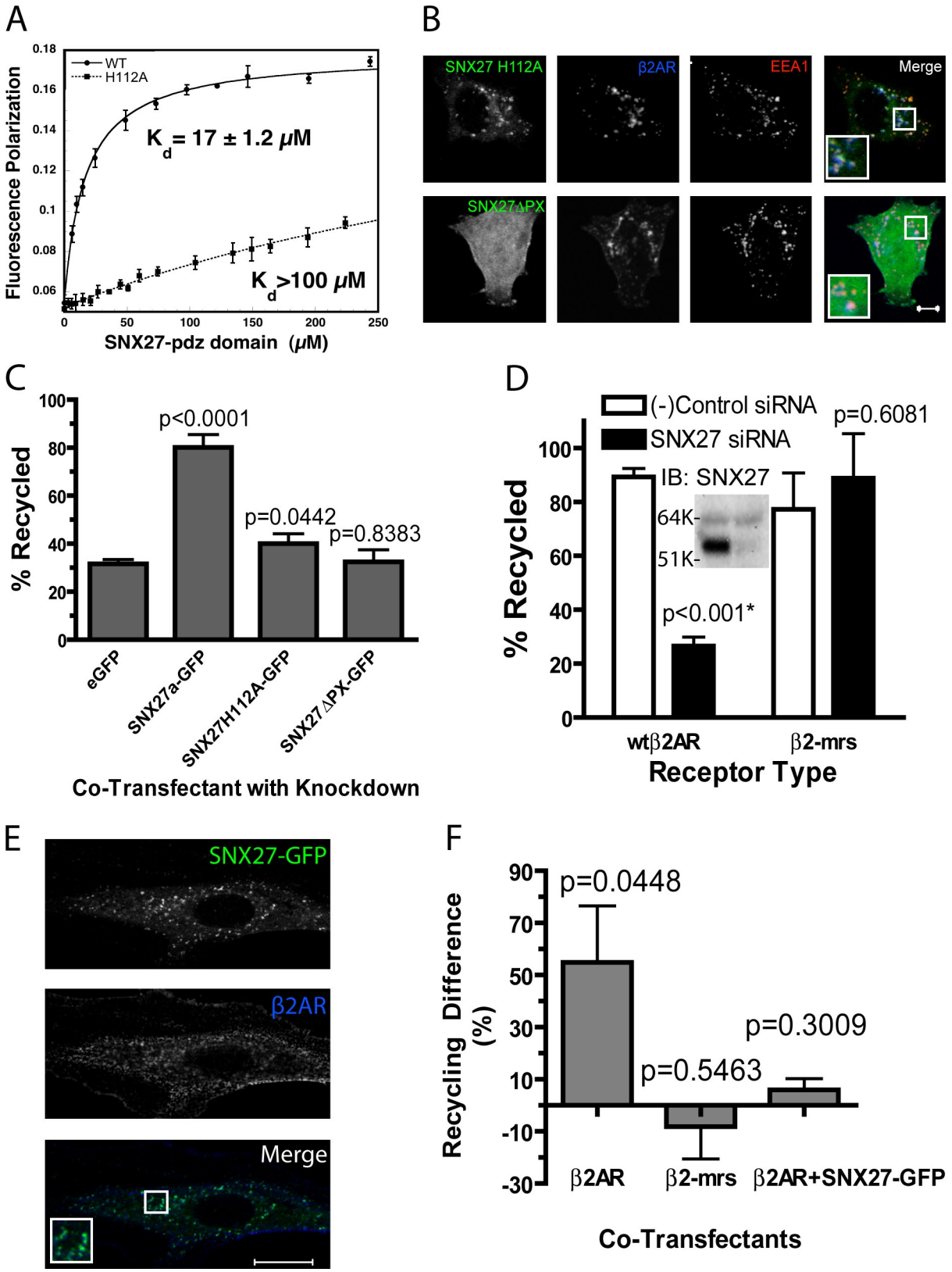

Figure 5. **The recycling activity of SNX27 requires both its PDZ domain–mediated interaction with cargo and PX domain–mediated association with endosomes.** (A) Fluorescence polarization analysis demonstrating the ability of the H112A mutation of the SNX27 PDZ domain to disrupt binding to the wild-type β_2AR-derived PDZ motif. Representative saturation plots for the wild-type PDZ domain (solid line) and H112A mutant PDZ domain (broken line) are shown. (B) Representative examples of fluorescence localization patterns of PDZ mutant (H112A) and PX mutant (ΔPX) versions of SNX27, relative to FLAG-β_2AR and EEA1, verifying that the PX domain is specifically required for early endosome localization of SNX27, whereas the PDZ domain is not. Bar, 5 µm. (C) Flow cytometric analysis of FLAG-β_2AR recycling in SNX27 knockdown cells also transfected with a GFP, SNX27a-GFP, or SNX27a-GFP containing a mutated PDZ domain (H112A) or deleted PX domain (ΔPX). Error bars indicate SEM. P-values: Student's *t* test comparison to the empty GFP control; $n = 4$.

detectably affect localization of the mutant SNX27 protein to early endosomes (Fig. 5 B, top; Pearson's coefficient = 0.55 ± 0.13; n = 29 images). However, the H112A mutant SNX27 was unable to rescue β_2AR recycling (Fig. 5 C, middle two bars). We also asked if SNX27's sorting activity requires its association with the endosome membrane. To do so, we used a mutant version of SNX27a possessing a wild-type PDZ domain but lacking the PX domain (SNX27ΔPX). SNX27ΔPX failed to localize to endocytic vesicles (Fig. 5 B, bottom; Pearson's coefficient = 0.19 ± 0.12; n = 20 images) and did not rescue the recycling defect caused by depletion of endogenous SNX27 (Fig. 5 C, rightmost bar). Together, these results indicate that the recycling activity of SNX27 requires both PDZ motif binding and direct association with the endosome membrane.

As an independent test of the specificity of SNX27 for PDZ-directed recycling, we examined the effect of replacing the PDZ motif present in the β_2AR cytoplasmic tail with a distinct 17-residue sequence derived from the cytoplasmic tail of the μ opioid neuropeptide receptor (Fig. S3 A). This μ receptor–derived recycling sequence (mrs) does not conform to a PDZ motif, and does not bind PDZ domains in vitro, but represents a PDZ-independent sorting motif that is sufficient to direct efficient recycling when substituted for the PDZ motif present in the wild-type β_2AR (Tanowitz and von Zastrow, 2003). β2-mrs recycling was insensitive to SNX27 knockdown (Fig. 5 D). SNX27 depletion also did not increase agonist-induced degradation of β2-mrs (Fig. S3, B and C). We further verified SNX27's localization and discrete sorting activity in a physiologically relevant cell type. SNX27 colocalized extensively with β_2AR-containing endosomes in aortic smooth muscle (A10) cells (Fig. 5 E; Pearson's coefficient = 0.58 ± 0.10; n = 6). Knockdown of endogenous SNX27 in these cells inhibited recycling of the β_2AR, but not the β2-mrs engineered receptor. Finally, this specific knockdown effect was rescued by recombinant SNX27 (Fig. 5 F).

Together, we believe that the present results provide several lines of evidence indicating that SNX27 is a critical sorting protein for PDZ motif–directed endosome-to-plasma membrane traffic, and that it mediates this sorting function directly from the endosome membrane. We note that the presently described function of SNX27 in PDZ-directed recycling is fundamentally different from the previously proposed roles of SNX27 in promoting endocytosis or lysosomal delivery of PDZ motif–bearing cargo (Joubert et al., 2004; Lunn et al., 2007). These previous studies relied entirely on the effects of SNX27 overexpression, and, consistent with this, we observed some agonist-independent accumulation of β_2ARs in endosomes when SNX27-GFP was overexpressed (Fig. S1 B, agonist-naive condition is shown in the bottom two rows). Depleting native SNX27 produced a much more pronounced retention of receptors in endosomes, however, which was evident under both agonist-induced (Fig. S2 C) and -naive (Fig. S1 C) conditions. Thus, although SNX27 overexpression can indeed produce additional effects consistent with expression-dependent differences in the functional effects of other sorting nexins (Carlton et al., 2005), we are confident that a primary function of SNX27 expressed endogenously is to promote PDZ motif–directed recycling from (rather than sequestration in) endosomes.

This function of SNX27 is also different from the roles of all other sorting nexins established previously. Sorting nexins are known to have a variety of effects on endocytic membrane organization and function, and several possess Bin/Amphiphysin/Rvs (BAR) domains that detect or impose membrane curvature. SNX27 lacks a recognized BAR domain, is the only known family member containing a PDZ domain, and, except for its PX domain, is largely distinct from other sorting nexins. It is interesting to note that sorting nexin 17 (SNX17), although it lacks a PDZ domain, shares homology with SNX27 elsewhere (Xu et al., 2001) and has been found to promote recycling of the low-density lipoprotein receptor–related protein (LRP) by interacting with a tyrosine-based sequence distinct from a PDZ motif (van Kerkhof et al., 2005). SNX27 could potentially function via PDZ-dependent inhibition of receptor interaction with the lysosomal sorting machinery or, alternatively, by promoting PDZ-directed packaging of receptors into recycling vesicles. The present data cannot distinguish these possibilities, but set the essential groundwork for further mechanistic elucidation of SNX27's discrete sorting activity.

We focused here on trafficking of the β_2AR because this was the integral membrane protein for which the hypothesis of PDZ-directed recycling was first proposed (Cao et al., 1999), because endosome-to-plasma membrane trafficking of this receptor is well established to have physiologically significant effects (Moore et al., 2007), and because there is emerging evidence that the PDZ-dependent recycling mechanism is conversely regulated by β_2AR signaling (Yudowski et al., 2009). We note that several other signaling receptors have been found to exhibit PDZ motif–dependent recycling (Wente et al., 2005; Delhaye et al., 2007; Hanyaloglu and von Zastrow, 2008). Further, PDZ domain–mediated protein interactions are recognized to function more widely in determining the endomembrane trafficking of various membrane proteins (e.g., Lin and Huganir, 2007;

(D) Flow cytometric analysis showing that SNX27 depletion specifically prevents PDZ motif–directed recycling of FLAG-β_2AR (first and second bars from the left; these data are replotted from Fig. 3 for comparison) without detectably affecting recycling directed by a distinct, non-PDZ sorting sequence (FLAG-β2-mrs, rightmost two bars). The inset shows a representative immunoblot confirming efficient knockdown of SNX27 in the FLAG-β2-mrs–expressing HEK293 cells used in the recycling assays (left lane, negative control; right lane, SNX27 siRNA transfection). K, kilodaltons. (E) SNX27-GFP and FLAG-β_2AR were coexpressed in A10 aortic smooth muscle cells. FLAG-β_2AR present in the plasma membrane was labeled and internalized as described in Materials and methods. Representative confocal images showing SNX27-GFP (top), FLAG-β_2AR (middle), and a merged image (bottom). Colocalization of SNX27-GFP with β_2AR-containing endosomes are enlarged 2× in the inset. Bar, 20 μm. (F) The effect of SNX27 depletion on FLAG-β_2AR or FLAG-β2-mrs recycling was measured in A10 cells by antibody efflux, as described in Materials and methods. Bars represent the reduction of recycling efficiency produced by SNX27 knockdown, measured 50 min after agonist removal from the culture medium. The third bar from the right shows a rescue condition, where the relative effect of SNX27 siRNA on FLAG-β_2AR recycling was assessed in the presence of recombinant SNX27. Error bars indicate SEM of recycling differences. P-values: paired t test of recycling percentage in negative control versus SNX27 siRNA-transfected conditions; n = 3–7.

Cushing et al., 2008; Maday et al., 2008; Wieman et al., 2009). We also note that the general concept of sequence-directed molecular sorting in the recycling pathway is now firmly established, particularly in polarized cell types (Mellman and Nelson, 2008). The molecular basis of such sorting has been studied most extensively in epithelial cells, where non-PDZ interactions of membrane cargo with AP-1B promote basolateral surface delivery involving Rab8 and components of the exocyst (Fölsch et al., 1999, 2003; Gan et al., 2002; Ang et al., 2003), and where such sorting has been shown to occur in recycling endosomes (Ang et al., 2004). We believe that the present study, by establishing SNX27 as a mediator of PDZ motif–directed recycling from the early endosome membrane, significantly extends the concept of molecular sorting in the recycling pathway and supports its physiological significance.

Materials and methods

Constructs and specialized reagents

Epitope-tagged receptor constructs have been described previously (von Zastrow and Kobilka, 1992; Cao et al., 1999; Tanowitz and von Zastrow, 2003). GFP-NHERF1 was generated from a previously described HA-tagged version of human EBP50/NHERF1 (Cao et al., 1999). The coding sequence was subcloned from pcDNA3.0 (Invitrogen) into pEGFP-C3 (Clontech) using XmnI and HindIII, and the C-terminal HA tag was removed by introduction of a stop codon using oligonucleotide site-directed mutagenesis (QuikChange; Agilent Technologies). GFP-NHERF2 was generated by PCR from a cDNA encoding human NHERF2/E3KARP (No. 5296143; Thermo Fisher Scientific). SNX27-GFP was generated from rat SNX27/mrt1 (isoform a, GenBank/EMBL/DDBJ accession No. NM_001110151, obtained from American Type Culture Collection) subcloned into pENTR.D.TOPO (Invitrogen). GFP tagging was accomplished by recombination into pcDNA-DEST47 (Gateway system; Invitrogen). The *b* isoform and the H112A mutant version were generated from SNX27-GFP using oligonucleotide site-directed mutagenesis. The ΔPX construct (deleting residues 162–263) was constructed using stitch PCR of the flanking sequence and insertion into the pENTR.D.TOPO vector followed by recombination into the pcDNA-DEST47 vector. For production of recombinant protein in *E. coli*, wild type or H112A mutant SNX27 PDZ domain (corresponding to residues 39–131 in the NM_001110151 coding sequence) were amplified by PCR and inserted using NcoI and XhoI sites to a pET19b-derived expression vector (pBH4) incorporating an N-terminal His_6 tag. All constructs were verified by dideoxynucleotide sequencing (Elim Biopharmaceuticals, Inc.). Control (nonsilencing) and silencing siRNAs were obtained from the HP GenomeWide siRNA collection (QIAGEN). The sense-strand, silencing siRNA sequences are as follows: NHERF1, 5′-GAAGGAGAACAGUCGUGAA(dTdT)-3′; NHERF2, 5′-GAGACAGAUGAACACUUCA(dTdT)-3′; and SNX27, 5′-CCAGGUAAUUGCAUUUGAA(dTdT)-3′. SNX27 silencing in rat A10 cells was accomplished with a mix of the four siRNAs available for that species commercially (HP GenomeWide siRNA collection, QIAGEN). To verify specific rescue in rat A10 cells, knockdown was achieved using 5′-GACCAAGUGUACCAGGCUA(dTdT)-3′ targeting endogenous SNX27, and this target sequence was removed from the SNX27 rescue construct by synonymous mutation (GTGTAC → GTATAT, nucleotides 1012–1017 of NM_001110151). Peptides corresponding to the C-terminal six residues of the β2AR (TNDSLL) and an alanine-extended version (TNDSLLA), labeled at the N terminus with fluorescein (FITC), were obtained from Genemed Synthesis. Monoclonal anti-FLAG antibody (M1; Sigma-Aldrich) was conjugated with Alexa Fluor dyes (Invitrogen) according to the manufacturer's instructions. Alexa Fluor–conjugated secondary antibodies were obtained from the same vendor. The dilutions and sources of other primary antibodies used were: 1:500 rabbit anti-FLAG (Sigma-Aldrich); 1:1,000 rabbit anti-EBP50 (ab3452; Abcam); 1:100 goat anti-NHERF2 (sc-21117; Santa Cruz Biotechnology, Inc.); 1:500 mouse anti-EEA1 (610457; BD); 1:500 mouse anti-LAMP3/CD63 (H5C6; Developmental Studies Hybridoma Bank, University of Iowa); and 1:100 rabbit anti-Rab11 (71–5300; Invitrogen). Anti-SNX27 mouse monoclonal IgG was generated using residues 1–267 of hSNX27 (Joubert et al., 2004) and used at a 1:1,000 dilution. HRP-coupled M2 antibody (Sigma-Aldrich) was used for receptor Westerns. HRP-coupled secondary antibodies were obtained from GE Healthcare (anti–mouse and anti–rabbit IgG) and Pierce (anti–goat IgG).

Cell culture and transfection

Human embryonic kidney 293 cells and A10 aortic smooth muscle cells (American Type Culture Collection) were maintained in DME supplemented with 10% fetal bovine serum (University of California, San Francisco Cell Culture Facility). NHERF-deficient PS120 cells were provided by M. Donowitz (Johns Hopkins University, Baltimore, MD). For siRNA transfection, cells at ∼30% confluency in 6-cm dishes were transfected with Lipofectamine RNAiMax (Invitrogen) and 40 pmol of siRNA according to the manufacturer's instructions, split into 12-well plates 48 h after transfection, and assayed at 72 h after transfection. For cotransfection of DNA and siRNA, Lipofectamine 2000 (Invitrogen) was used with 40 pmol siRNA and ∼2 µg DNA in the same plating format and recommended protocol. DNA transfection was performed in 6-well or 12-well plates at ∼50% cell confluency using Lipofectamine 2000 according to the manufacturer's instructions. Stably transfected cells were selected in 500 µg/ml Geneticin (Life Technologies), and cell clones expressing FLAG-tagged receptor constructs were chosen at similar levels based on mean surface immunofluorescence/cell measured through flow cytometry, and found to have at least 90% of cells expressing surface immunoreactivity. Radioligand binding assay (performed as described in the next paragraph) verified that total receptor expression in each clone was in the range of 2–4 pmol/mg protein.

Radioligand binding assays

A single-point radioligand binding assay to estimate total receptor expression was performed using a minor variation of a previously described method (von Zastrow and Kobilka, 1992). In brief, cells plated in 6-well dishes were washed with PBS, exposed to one cycle of freezing (−20°C) and thawing, and mechanically resuspended in 200 µl PBS. Equal amounts of cell lysate (50–100 µg total protein as determined by a Bradford assay) were aliquoted into 96-well plates and brought to a total volume of 100 µl PBS including 11.5 nM [^{3}H]dihydroalprenolol (GE Healthcare), a saturating concentration used to estimate B_{max}. Each lysate was assayed in triplicate, and nonspecific binding was determined by including 10 µM of unlabeled alprenolol (Sigma-Aldrich). Plates were incubated for 1 h at room temperature with shaking, and membranes were harvested by filtration binding through glass fiber (GF/C; GE Healthcare) using a vacuum-driven harvester (Filtermate 196; Packard Instruments). Filters were washed extensively with 20 mM Tris Cl, pH 7.5, and bound radioactivity was determined by liquid scintillation counting (TriCarb 2100TR; Packard Instruments).

Fluorescence polarization assays

Wild-type and H112A mutant PDZ domains derived from SNX27, cloned in pBH4, were transformed into *E. coli* strain BL21(DE3) pLYS-S for expression, and recombinant proteins were purified using a Ni^{2+}-NTA (QIAGEN) column. Proteins were further purified on a 16/60 Sephacryl S-100 gel filtration column (GE) run in 20 mM Hepes/100 mM NaCl, pH 7.4. The purified proteins were concentrated to 600–800 µM, frozen in liquid nitrogen, and stored at −80°C. Concentrations were determined using the Bradford method. The binding of the N-terminal fluorescein-labeled peptides (TNDSLL and TNDSLLA) was monitored by following the increase in fluorescence polarization upon titration of the concentrated PDZ domain. The assay was performed in 384-well plates containing 10 nM of labeled peptide in each well. The experiments were performed in 20 mM Hepes, pH 7.4, 100 mM NaCl, and 20 mM DTT at room temperature. Fluorescence polarization was measured using an Analyst HT Fluorometer (Molecular devices) with excitation and emission set to 485 nm and 530 nm, respectively (Harris et al., 2001).

Fluorescence microscopy

To assess localization of β_2ARs, PDZ proteins, and/or endosomal markers in HEK293 cells stably expressing FLAG-tagged β_2AR, cells were transfected with siRNA or constructs encoding GFP-tagged PDZ protein where appropriate. 48 h later, agonist-naive cells were incubated in the presence of Alexa Fluor 647–conjugated M1 anti-FLAG antibody (10 µg/ml) or rabbit anti-FLAG antibody (2 µg/ml) for 20 min to selectively label β_2ARs present in the plasma membrane. To label the internalized receptor pool, cells were subsequently incubated for 25 min in the presence of 10 µM isoproterenol, a condition that is sufficient to drive labeled β_2ARs to steady state in the recycling pathway. Cells were then quickly washed with cold PBS and fixed in 4% formaldehyde/PBS for 10 min at room temperature, followed by a Tris-buffered saline quench for 5 min. Cells were then permeabilized where needed for 20 min in 0.1% Triton-X 100 and 5%

FBS in PBS before primary and secondary antibody staining in the same buffer for 1 h each. A10 cells were transfected with receptor constructs and additional oligonucleotide as indicated, and labeled for FLAG-tagged receptors similarly. Surface-accessible Alexa Fluor 647–conjugated M1 antibody was further labeled with Alexa Fluor 555–conjugated anti–mouse IgG at 4°C before fixation. Fixed specimens were mounted to glass slides in Fluormount-G (SouthernBiotech) and examined at room temperature. Laser-scanning confocal microscopy was performed using a microscope (LSM510; Carl Zeiss, Inc.) fitted with a 63×/NA 1.4 oil objective lens. Wide-field (epifluorescence) microscopy was performed using a microscope (Diaphot; Nikon) equipped with a 60×/NA 1.4 oil objective lens, mercury arc lamp, standard dichroic filter sets (Chroma Technology Corp.), and a 12-bit cooled charge-coupled device camera (MicroMax; Princeton Instruments) interfaced to a computer running MetaMorph acquisition and analysis software (MDS Analytical Technologies). Wide-field images were rendered using ImageJ (http://rsb.info.nih.gov/ij/; Collins, 2007) and confocal images were rendered using LSM software (Carl Zeiss, Inc.). Illustrations were prepared using Photoshop and Illustrator software (Adobe). Background subtraction and scaling were performed using nonsaturated images and linear lookup tables. Colocalization analysis was assessed in confocal optical sections in two ways. First, independent scoring of positive structures in SNX27, EEA1, or receptor channels was done visually, with manual counting. Positive structures were defined by fluorescence intensity at least three standard deviations above background and encompassing contiguous pixels representing at least 500 nm. Degree of overlap was calculated from individual images and averaged over the indicated number of specimens selected at random. Second, colocalization was estimated by calculating the Pearson's correlation coefficient between the indicated image channels using the Manders_Coefficients.java plugin for ImageJ (T. Collins and W. Rasband, Wright Cell Imaging Facility, Toronto Western Research Institute, and National Institutes of Health, Bethesda, MD).

Fluorescence flow cytometry

Internalization and recycling of FLAG-tagged receptor constructs was assessed using Alexa Fluor 647–conjugated M1 anti-FLAG antibody and a FACSCalibur flow cytometer (BD) as described previously (Hanyaloglu and von Zastrow, 2007). Internalization was determined by reduction of surface receptor immunoreactivity observed after incubation of cells in the presence of the adrenergic agonist isoproterenol (10 µM) for the indicated number of minutes at 37°C. Recycling in HEK293 cells was determined by recovery of surface receptor immunoreactivity measured after a 25-min exposure to isoproterenol and a subsequent agonist-removal incubation (50 min unless indicated otherwise) in the presence of the adrenergic antagonist alprenolol (10 µM) to prevent any residual agonist effects (corresponding to the ALP segment in Fig. 1 C). Analysis of recycling data according to the level of recombinant SNX27 expression was performed using dual-channel flow cytometry in cells transiently transfected with the indicated version of SNX27-GFP, also as described previously (Lauffer et al., 2009). Recycling in A10 smooth muscle cells was evaluated by internalizing Alexa Fluor 647–conjugated M1 antibody with receptors as described above for microscopy experiments, and determining internal receptor fluorescence loss after a 50-min agonist withdrawal incubation and subsequent cell dissociation (TrypLE trypsin replacement buffer; Invitrogen) at 4°C to retain internalized fluorescent antibodies while removing surface-accessible ones. Each experiment used duplicate or triplicate determinations of 2–10,000 cells each, and results shown represent the receptor recycling in cells transfected with negative control siRNA minus that seen in cells transfected with SNX27 siRNA.

Western blot analysis

To assess knockdown efficiency, duplicate wells from the indicated analysis performed in a 12-well plate were combined and solubilized in 200 µl of lysis buffer: 0.1% (vol/vol) Triton X-100, 150 mM NaCl, 25 mM KCl, 10 mM Tris, pH 7.4, and complete protease inhibitor cocktail (Roche). Lysates were clarified by centrifugation for 10 min at 20,000 *g* in a microcentrifuge, the protein concentration of extracts was determined using a Bradford assay, and equal protein loads were mixed 3:1 with 4× LDS sample buffer (Invitrogen) supplemented with 5% β-mercaptoethanol before heating to 95°C for 5 min. Biotin-labeled, GPCR degradation assays have been described previously (Gage et al., 2001), and were used here for isolation of mature receptor via surface protein biotinylation, streptavidin-agarose precipitation, and anti-FLAG immunoblotting. Protein samples from these experiments were reduced and denatured at 37°C for 1 h. The solubilized extracts were separated by SDS-PAGE, transferred to nitrocellulose, and Ponceau S stained to verify equal loading before immunoblotting. Antibody incubations were performed for 1 h at room temperature in TBST containing 5% milk or BSA (anti-NHERF2). Immunoreactive species were identified using HRP-conjugated secondary antibodies (1:3,000) or HRP-conjugated M2 antibody (1:500) followed by chemiluminescence detection (SuperSignal; Thermo Fisher Scientific). Exposures were captured using x-ray film or, for quantitative assessment, using a FluorChem 8000 luminescence imaging system (Cell Biosciences).

Statistical and kinetic analysis

In flow cytometric assays, mean fluorescence/cell of duplicate or triplicate collections of cells were used to calculate relative changes in basal surface receptor expression, agonist-induced internalization, and recycling efficiency for each independent experiment. Integrated densities of receptor–antibody–HRP luminescence in individual samples from biotin degradation immunoblots were similarly normalized to the indicated reference for each independent experiment. Data were collected as replicates in a Prism spreadsheet for statistical and graphing analysis (GraphPad Software, Inc.). Replicate values were compared with the given reference using a Student's *t* test or paired *t* test as indicated in the figure legends. Curve fitting of internalization and recycling time courses used replicate percentages over the multiple time points indicated to generate rate constants according to a two-compartment endocytic recycling model. The rate of recycling was described by recycling % = $F_r(1 - e^{-kr t})$ and the internalization kinetics were described by $F_{SR} = [F_r\, k_r + k_e \times e^{-(ke + Fr\, kr)t}]/[ke + Fr\, kr]$, where F_r is the recycling efficiency or maximum fraction recycled, k_r is the recycling rate constant, t is the time in minutes, F_{SR} is the fraction of surface receptor remaining, and k_e is the endocytic rate constant. Fitting of triplicate fluorescence polarization values of peptides to increasing concentrations of PDZ protein using a single binding site model have been described previously (Harris et al., 2001).

Online supplemental material

Fig. S1 shows subcellular localization of FLAG-β_2AR and PDZ-interacting proteins in agonist-naive and agonist-exposed HEK293 cells, and the recycling defect of SNX27 depletion, as visualized by fluorescence microscopy. Fig. S2 shows the effects of PDZ protein knockdowns on steady-state receptor expression and internalization. Fig. S3 shows a schematic of the FLAG-β_2AR-mrs construct, and that its down-regulation is insensitive to SNX27 knockdown. Online supplemental material is available at http://www.jcb.org/cgi/content/full/jcb.201004060/DC1.

We thank Henry Bourne, Robert Edwards, Keith Mostov, and Bill Thelin for useful discussions, Mark Donowitz for providing PS120 cells, and Courtni Salinas for assistance in developing critical reagents. The Laboratory for Cellular Analysis of the Hellen Diller Family Comprehensive Cancer Center at University of California, San Francisco, administered flow cytometry and confocal microscopy instrumentation.

These studies were supported by the National Institutes of Health (NIH DA012864 and DA010711 to M. von Zastrow) and the National Institutes of Health Roadmap for Medical Research (PN2 EY016546 to T. Kortemme).

Submitted: 12 April 2010
Accepted: 25 July 2010

References

Ang, A.L., H. Fölsch, U.M. Koivisto, M. Pypaert, and I. Mellman. 2003. The Rab8 GTPase selectively regulates AP-1B-dependent basolateral transport in polarized Madin-Darby canine kidney cells. *J. Cell Biol.* 163:339–350. doi:10.1083/jcb.200307046

Ang, A.L., T. Taguchi, S. Francis, H. Fölsch, L.J. Murrells, M. Pypaert, G. Warren, and I. Mellman. 2004. Recycling endosomes can serve as intermediates during transport from the Golgi to the plasma membrane of MDCK cells. *J. Cell Biol.* 167:531–543. doi:10.1083/jcb.200408165

Appleton, B.A., Y. Zhang, P. Wu, J.P. Yin, W. Hunziker, N.J. Skelton, S.S. Sidhu, and C. Wiesmann. 2006. Comparative structural analysis of the Erbin PDZ domain and the first PDZ domain of ZO-1. Insights into determinants of PDZ domain specificity. *J. Biol. Chem.* 281:22312–22320. doi:10.1074/jbc.M602901200

Bretscher, A., D. Chambers, R. Nguyen, and D. Reczek. 2000. ERM-Merlin and EBP50 protein families in plasma membrane organization and function. *Annu. Rev. Cell Dev. Biol.* 16:113–143. doi:10.1146/annurev.cellbio.16.1.113

Cao, T.T., H.W. Deacon, D. Reczek, A. Bretscher, and M. von Zastrow. 1999. A kinase-regulated PDZ-domain interaction controls endocytic sorting of the beta2-adrenergic receptor. *Nature.* 401:286–290. doi:10.1038/45816

Carlton, J., M. Bujny, A. Rutherford, and P. Cullen. 2005. Sorting nexins—unifying trends and new perspectives. *Traffic.* 6:75–82. doi:10.1111/j.1600-0854.2005.00260.x

Collins, T.J. 2007. ImageJ for microscopy. *Biotechniques.* 43:25–30. doi:10.2144/000112517

Cushing, P.R., A. Fellows, D. Villone, P. Boisguérin, and D.R. Madden. 2008. The relative binding affinities of PDZ partners for CFTR: a biochemical basis for efficient endocytic recycling. *Biochemistry.* 47:10084–10098. doi:10.1021/bi8003928

Delhaye, M., A. Gravot, D. Ayinde, F. Niedergang, M. Alizon, and A. Brelot. 2007. Identification of a postendocytic sorting sequence in CCR5. *Mol. Pharmacol.* 72:1497–1507. doi:10.1124/mol.107.038422

Donowitz, M., B. Cha, N.C. Zachos, C.L. Brett, A. Sharma, C.M. Tse, and X. Li. 2005. NHERF family and NHE3 regulation. *J. Physiol.* 567:3–11. doi:10.1113/jphysiol.2005.090399

Doyle, D.A., A. Lee, J. Lewis, E. Kim, M. Sheng, and R. MacKinnon. 1996. Crystal structures of a complexed and peptide-free membrane protein-binding domain: molecular basis of peptide recognition by PDZ. *Cell.* 85:1067–1076. doi:10.1016/S0092-8674(00)81307-0

Fölsch, H., H. Ohno, J.S. Bonifacino, and I. Mellman. 1999. A novel clathrin adaptor complex mediates basolateral targeting in polarized epithelial cells. *Cell.* 99:189–198. doi:10.1016/S0092-8674(00)81650-5

Fölsch, H., M. Pypaert, S. Maday, L. Pelletier, and I. Mellman. 2003. The AP-1A and AP-1B clathrin adaptor complexes define biochemically and functionally distinct membrane domains. *J. Cell Biol.* 163:351–362. doi:10.1083/jcb.200309020

Gage, R.M., K.A. Kim, T.T. Cao, and M. von Zastrow. 2001. A transplantable sorting signal that is sufficient to mediate rapid recycling of G protein-coupled receptors. *J. Biol. Chem.* 276:44712–44720. doi:10.1074/jbc.M107417200

Gage, R.M., E.A. Matveeva, S.W. Whiteheart, and M. von Zastrow. 2005. Type I PDZ ligands are sufficient to promote rapid recycling of G Protein-coupled receptors independent of binding to N-ethylmaleimide-sensitive factor. *J. Biol. Chem.* 280:3305–3313. doi:10.1074/jbc.M406934200

Gan, Y., T.E. McGraw, and E. Rodriguez-Boulan. 2002. The epithelial-specific adaptor AP1B mediates post-endocytic recycling to the basolateral membrane. *Nat. Cell Biol.* 4:605–609.

Gardner, L.A., A.P. Naren, and S.W. Bahouth. 2007. Assembly of an SAP97-AKAP79-cAMP-dependent protein kinase scaffold at the type 1 PSD-95/DLG/ZO1 motif of the human beta(1)-adrenergic receptor generates a receptosome involved in receptor recycling and networking. *J. Biol. Chem.* 282:5085–5099. doi:10.1074/jbc.M608871200

Gouet, P., E. Courcelle, D.I. Stuart, and F. Métoz. 1999. ESPript: analysis of multiple sequence alignments in PostScript. *Bioinformatics.* 15:305–308. doi:10.1093/bioinformatics/15.4.305

Hall, R.A., R.T. Premont, C.W. Chow, J.T. Blitzer, J.A. Pitcher, A. Claing, R.H. Stoffel, L.S. Barak, S. Shenolikar, E.J. Weinman, et al. 1998. The beta2-adrenergic receptor interacts with the Na+/H+-exchanger regulatory factor to control Na+/H+ exchange. *Nature.* 392:626–630. doi:10.1038/33458

Hanyaloglu, A.C., and M. von Zastrow. 2007. A novel sorting sequence in the beta2-adrenergic receptor switches recycling from default to the Hrs-dependent mechanism. *J. Biol. Chem.* 282:3095–3104. doi:10.1074/jbc.M605398200

Hanyaloglu, A.C., and M. von Zastrow. 2008. Regulation of GPCRs by endocytic membrane trafficking and its potential implications. *Annu. Rev. Pharmacol. Toxicol.* 48:537–568. doi:10.1146/annurev.pharmtox.48.113006.094830

Hanyaloglu, A.C., E. McCullagh, and M. von Zastrow. 2005. Essential role of Hrs in a recycling mechanism mediating functional resensitization of cell signaling. *EMBO J.* 24:2265–2283. doi:10.1038/sj.emboj.7600688

Harris, B.Z., B.J. Hillier, and W.A. Lim. 2001. Energetic determinants of internal motif recognition by PDZ domains. *Biochemistry.* 40:5921–5930. doi:10.1021/bi0101421

He, J., M. Bellini, H. Inuzuka, J. Xu, Y. Xiong, X. Yang, A.M. Castleberry, and R.A. Hall. 2006. Proteomic analysis of beta1-adrenergic receptor interactions with PDZ scaffold proteins. *J. Biol. Chem.* 281:2820–2827. doi:10.1074/jbc.M509503200

Joubert, L., B. Hanson, G. Barthet, M. Sebben, S. Claeysen, W. Hong, P. Marin, A. Dumuis, and J. Bockaert. 2004. New sorting nexin (SNX27) and NHERF specifically interact with the 5-HT4a receptor splice variant: roles in receptor targeting. *J. Cell Sci.* 117:5367–5379. doi:10.1242/jcs.01379

Kajii, Y., S. Muraoka, S. Hiraoka, K. Fujiyama, A. Umino, and T. Nishikawa. 2003. A developmentally regulated and psychostimulant-inducible novel rat gene mrt1 encoding PDZ-PX proteins isolated in the neocortex. *Mol. Psychiatry.* 8:434–444. doi:10.1038/sj.mp.4001258

Lauffer, B.E., S. Chen, C. Melero, T. Kortemme, M. von Zastrow, and G.A. Vargas. 2009. Engineered protein connectivity to actin mimics PDZ-dependent recycling of G protein-coupled receptors but not its regulation by Hrs. *J. Biol. Chem.* 284:2448–2458. doi:10.1074/jbc.M806370200

Lin, D.-T., and R.L. Huganir. 2007. PICK1 and phosphorylation of the glutamate receptor 2 (GluR2) AMPA receptor subunit regulates GluR2 recycling after NMDA receptor-induced internalization. *J. Neurosci.* 27:13903–13908. doi:10.1523/JNEUROSCI.1750-07.2007

Lunn, M.-L., R. Nassirpour, C. Arrabit, J. Tan, I. McLeod, C.M. Arias, P.E. Sawchenko, J.R. Yates III, and P.A. Slesinger. 2007. A unique sorting nexin regulates trafficking of potassium channels via a PDZ domain interaction. *Nat. Neurosci.* 10:1249–1259. doi:10.1038/nn1953

Maday, S., E. Anderson, H.C. Chang, J. Shorter, A. Satoh, J. Sfakianos, H. Fölsch, J.M. Anderson, Z. Walther, and I. Mellman. 2008. A PDZ-binding motif controls basolateral targeting of syndecan-1 along the biosynthetic pathway in polarized epithelial cells. *Traffic.* 9:1915–1924. doi:10.1111/j.1600-0854.2008.00805.x

Marchese, A., M.M. Paing, B.R.S. Temple, and J. Trejo. 2008. G protein-coupled receptor sorting to endosomes and lysosomes. *Annu. Rev. Pharmacol. Toxicol.* 48:601–629. doi:10.1146/annurev.pharmtox.48.113006.094646

Maxfield, F.R., and T.E. McGraw. 2004. Endocytic recycling. *Nat. Rev. Mol. Cell Biol.* 5:121–132. doi:10.1038/nrm1315

Mellman, I., and W.J. Nelson. 2008. Coordinated protein sorting, targeting and distribution in polarized cells. *Nat. Rev. Mol. Cell Biol.* 9:833–845. doi:10.1038/nrm2525

Moore, C.A.C., S.K. Milano, and J.L. Benovic. 2007. Regulation of receptor trafficking by GRKs and arrestins. *Annu. Rev. Physiol.* 69:451–482. doi:10.1146/annurev.physiol.69.022405.154712

Perego, C., C. Vanoni, A. Villa, R. Longhi, S.M. Kaech, E. Fröhli, A. Hajnal, S.K. Kim, and G. Pietrini. 1999. PDZ-mediated interactions retain the epithelial GABA transporter on the basolateral surface of polarized epithelial cells. *EMBO J.* 18:2384–2393. doi:10.1093/emboj/18.9.2384

Rincón, E., T. Santos, A. Avila-Flores, J.P. Albar, V. Lalioti, C. Lei, W. Hong, and I. Mérida. 2007. Proteomics identification of sorting nexin 27 as a diacylglycerol kinase zeta-associated protein: new diacylglycerol kinase roles in endocytic recycling. *Mol. Cell. Proteomics.* 6:1073–1087. doi:10.1074/mcp.M700047-MCP200

Tanowitz, M., and M. von Zastrow. 2003. A novel endocytic recycling signal that distinguishes the membrane trafficking of naturally occurring opioid receptors. *J. Biol. Chem.* 278:45978–45986. doi:10.1074/jbc.M304504200

Thompson, J.D., D.G. Higgins, and T.J. Gibson. 1994. CLUSTAL W: improving the sensitivity of progressive multiple sequence alignment through sequence weighting, position-specific gap penalties and weight matrix choice. *Nucleic Acids Res.* 22:4673–4680. doi:10.1093/nar/22.22.4673

Tonikian, R., Y. Zhang, S.L. Sazinsky, B. Currell, J.-H. Yeh, B. Reva, H.A. Held, B.A. Appleton, M. Evangelista, Y. Wu, et al. 2008. A specificity map for the PDZ domain family. *PLoS Biol.* 6:e239. doi:10.1371/journal.pbio.0060239

van Kerkhof, P., J. Lee, L. McCormick, E. Tetrault, W. Lu, M. Schoenfish, V. Oorschot, G.J. Strous, J. Klumperman, and G. Bu. 2005. Sorting nexin 17 facilitates LRP recycling in the early endosome. *EMBO J.* 24:2851–2861. doi:10.1038/sj.emboj.7600756

von Zastrow, M., and B.K. Kobilka. 1992. Ligand-regulated internalization and recycling of human beta 2-adrenergic receptors between the plasma membrane and endosomes containing transferrin receptors. *J. Biol. Chem.* 267:3530–3538.

Wang, Y., B. Lauffer, M. Von Zastrow, B.K. Kobilka, and Y. Xiang. 2007. N-ethylmaleimide-sensitive factor regulates beta2 adrenoceptor trafficking and signaling in cardiomyocytes. *Mol. Pharmacol.* 72:429–439. doi:10.1124/mol.107.037747

Wente, W., T. Stroh, A. Beaudet, D. Richter, and H.-J. Kreienkamp. 2005. Interactions with PDZ domain proteins PIST/GOPC and PDZK1 regulate intracellular sorting of the somatostatin receptor subtype 5. *J. Biol. Chem.* 280:32419–32425. doi:10.1074/jbc.M507198200

Wieman, H.L., S.R. Horn, S.R. Jacobs, B.J. Altman, S. Kornbluth, and J.C. Rathmell. 2009. An essential role for the Glut1 PDZ-binding motif in growth factor regulation of Glut1 degradation and trafficking. *Biochem. J.* 418:345–367. doi:10.1042/BJ20081422

Xu, Y., L.F. Seet, B. Hanson, and W. Hong. 2001. The Phox homology (PX) domain, a new player in phosphoinositide signalling. *Biochem. J.* 360:513–530. doi:10.1042/0264-6021:3600513

Yudowski, G.A., M.A. Puthenveedu, A.G. Henry, and M. von Zastrow. 2009. Cargo-mediated regulation of a rapid Rab4-dependent recycling pathway. *Mol. Biol. Cell.* 20:2774–2784. doi:10.1091/mbc.E08-08-0892